AD-A232 244

MARYLAND

COLLEGE PARK CAMPUS

THE PROBLEM OF MODELING THE ELASTOMECHANICS IN ENGINEERING

Ivo Babuška
Institute for Physical Science and Technology
University of Maryland
College Park, MD 20742 USA

BN-1108

DTIC
ELECTE
MAR 0 6 1991
S B D

February 1990

INSTITUTE FOR PHYSICAL SCIENCE AND TECHNOLOGY

REPORT DOCUMENTATION PAGE		READ INSTRUCTIONS BEFORE COMPLETING FORM
1. REPORT NUMBER Technical Note BN-1108	2. GOVT ACCESSION NO.	3. RECIPIENT'S CATALOG NUMBER
4. TITLE (and Subtitle) The Problem of Modeling the Elastomechanics in Engineering		5. TYPE OF REPORT & PERIOD COVERED Final life of contract
		6. PERFORMING ORG. REPORT NUMBER
7. AUTHOR(s) Ivo Babuska		8. CONTRACT OR GRANT NUMBER(s) ONR/N00014-89-J-1030 NSF/CCR-88-20279
9. PERFORMING ORGANIZATION NAME AND ADDRESS Institute for Physical Science and Technology University of Maryland College Park, MD 20742		10. PROGRAM ELEMENT, PROJECT, TASK AREA & WORK UNIT NUMBERS
11. CONTROLLING OFFICE NAME AND ADDRESS Department of the Navy Office of Naval Research Arlington, VA 22217		12. REPORT DATE February 1990
		13. NUMBER OF PAGES 43
14. MONITORING AGENCY NAME & ADDRESS(if different from Controlling Office)		15. SECURITY CLASS. (of this report)
		15a. DECLASSIFICATION/DOWNGRADING SCHEDULE

16. DISTRIBUTION STATEMENT (of this Report)

Approved for public release: distribution unlimited

17. DISTRIBUTION STATEMENT (of the abstract entered in Block 20, if different from Report)

18. SUPPLEMENTARY NOTES

19. KEY WORDS (Continue on reverse side if necessary and identify by block number)

20. ABSTRACT (Continue on reverse side if necessary and identify by block number)

The paper describes the major aspects of modelling engineering problems of elastomechanics. It shows various aspects and results on a set of illustrative examples of 2 and 3 dimensional problems.

DD FORM 1473 EDITION OF 1 NOV 65 IS OBSOLETE
1 JAN 73

S/N 0102-LF-014-6601

The Problem of Modeling the Elastomechanics in Engineering

Ivo Babuˇska
Institute for Physical Science and Technology
University of Maryland
College Park, MD 20742 USA

Abstract

The paper describes the major aspects of modeling engineering problems of elastomechanics. It shows various aspects and results on a set of illustrative examples of 2 and 3 dimensional problems.

Accession For		
NTIS GRA&I	☑	
DTIC TAB	☐	
Unannounced	☐	
Justification		
By		
Distribution/		
Availability Codes		
Dist	Avail and/or Special	
A-1		

1. Introduction

The aim of computational analysis is to describe and *reliably predict* physical phenomena of interest. In the engineering sciences the primary aim is usually to design tools which operate SAFELY under certain (mechanical) conditions, in certain environments and for a certain period of time.

By computational analysis, ONLY mathematical problems and NOT the reality can be analyzed. The mathematical problem TRANSFORMS given input data into information which is of direct interest and does not add anything new (in fact its loses some information).

The aim of computation is to reliably obtain certain information in the range of an admissible tolerance so that it is not unduly influenced by the computational procedure used.

The formulation of the mathematical problem is usually the most crucial part of the analysis. Because of the complexity of engineering analysis and uncertainties in the available information, the formulation of the mathematical problem is often directly or indirectly stipulated in the design codes and often (at least in parts) it is also influenced by the particular (company) engineering practices. These codes change with time and express the experiences with the technology used. As a typical example we mention the design code (USAF-MIL-A-83444) used in aircraft components. It is based on the principle of "non-inspectable slow crack growth" which should meet the following demands

a) the life of the component should exceed two design times

b) the residual strength of the component should, after being in service two design life time, exceed maximal load acting on the component by a factor of, say, 9/8.

3

These or similar principles and other considerations (for example, un-
certainties in the input information) lead to the *precise formulation of the*
mathematical problem and defining the data which have to be obtained as well
as to the admissible accuracy with which they have to be determined.

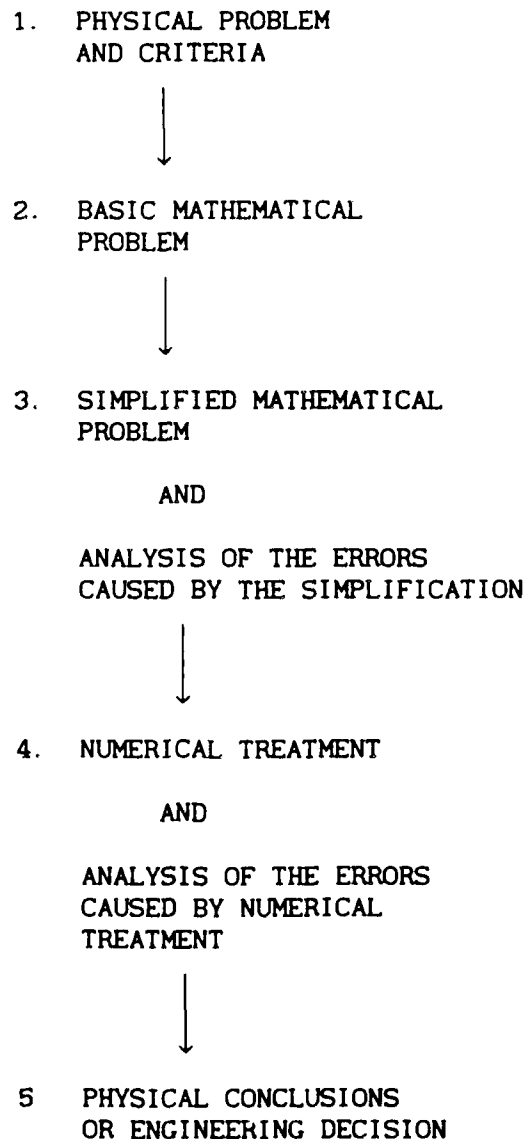The basic flow chart of an engineering computational analysis is shown
in Fig. 1.

1. PHYSICAL PROBLEM
    AND CRITERIA

          ↓

2. BASIC MATHEMATICAL
    PROBLEM

          ↓

3. SIMPLIFIED MATHEMATICAL
    PROBLEM

       AND

    ANALYSIS OF THE ERRORS
    CAUSED BY THE SIMPLIFICATION

          ↓

4. NUMERICAL TREATMENT

       AND

    ANALYSIS OF THE ERRORS
    CAUSED BY NUMERICAL
    TREATMENT

          ↓

5   PHYSICAL CONCLUSIONS
    OR ENGINEERING DECISION

Fig. 1.   The flow chart of computational analysis.

4

Usually in practice loops are present in the flow chart.

The "reality" is associated with (1). The engineering analysis of the problem, the aims of the analysis, and the assessement of the quality of the available data. etc. then yield the precisely formulated mathematical problem (model) (2). This model is to be understood as a "higher" model *which is identified with reality*. Nevertheless we solve usually only a simplified problem (3) and reliability of its solution is judged typically in comparison with (2). In (4) we solve numerically problem (3) and the reliability and the error of the numerical solution is related to the (exact) solution of (3) (and not (2) or (1)).

Let us underline that basic and simplified mathematical problem has to have reasonable mathematical properties, for example the existence of a solution. The existence of the solution of the "real" problem does not necessarily mean that the solution of the *mathematical problem* exists too. This is because of the simplification which enters into the formulation of the mathematical problem. Also, if the numerical algorithm provides numerical results (possibly reasonable looking), it does not mean that the solution of the mathematical problem necessarily exists, (because convergence has not to occur etc.) Obviously, theoretical analysis of the mathematical problem and comparison of its properties with the expected properties of the reality is essential part of the reliability of the model.

In all stages we have to relate the numerically obtained solution to the exact solution of a mathematical problem. The agreement with reality, for example with experiments, is then related solely to the formulation of the basic (or possibly simplified) problem. It is essential that the errors of numerical solutions are completely under control so that the exact solution of the mathematical problem is essentially achieved and a possible disagreement

with experiments is related ONLY to the mathematical problem itself.

In this paper we will show various concrete examples to illustrate the basic ideas and results. All the computations in this paper has been made by the h-p version of the finite element method by the code PROBE (McNeil Schwendler-Noetic) and STRIPE (Aeronautical Institute of Sweden). These codes have various error checks so that the numerical results presented here can be assumed to be exact in the range of accuracy needed for the model conclusions.

2) Problem of the cantilever beam

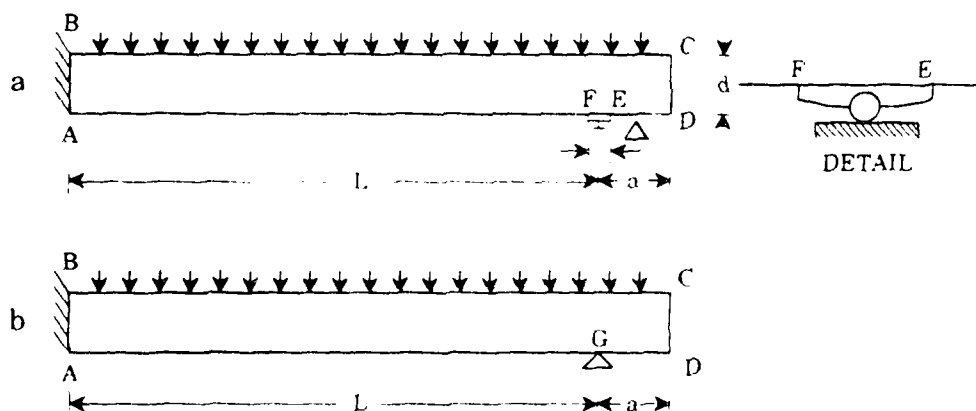Consider a problem of a simply supported cantilever beam shown in Fig.2.1a

Fig.2.1 The simply supported cantilever beam

Let *the basic mathematical problem* be the problem of two dimensional linear elasticity (plane strain) for isotropic homogeneous material. The basic unknowns, the displacement u, v, satisfy the usual Lamé-Navier equations of elasticity. As the boundary conditions shown in the Fig.2.1a. we impose on $\overline{BC}: T_y = p, T_x = 0$, on $\overrightarrow{AB}, u = v = 0$, on $\overline{CD}, \overline{DE}, \overline{FA}: T_x = T_y = 0$ and on $\overline{EF}$ (where $\Delta \ll d) T_x = 0, v = b(x-L')$ where b is such that $\int_{EF} T_y(x-L')dx = 0$.

By T_x respect to T_y we denoted the tractions. The problem is a model of the simply supported cantilever beam. The (weak) solution which has finite energy *exists and is uniquely determined.*

Let us now consider the *simplified problem* when $\Delta = 0$ and when $v = 0$ at the point G (see Fig.2.1b) is prescribed instead of the more complicated boundary condition of the basic problem. Then it is possible to show that the unique (weak) solution of the *simplified problem is the same* as the one when the condition $v = 0$ at G *is not present.* We see that the solution of the simplified problem is unacceptable. The reason for it is that the displacement under concentrated load is infinite (the Bousinesque solution). Although the solutions of the basic problem converges to the simplified one as $\Delta \rightarrow 0$, the convergence *is very slow* and so it is inadmissible to consider this limiting case instead of the original one.

We remark that the point support is standardly used in finite element computations, i.e. the simplified problem is often numerically solved. Hence the error of the finite element solution is very large because for a mesh not extremely refined the cantilever beam solution without support, i.e. the exact solution is not obtained. It is possible to show that the finite element solution converges to the solution for the beam without support as the mesh size converges to zero. Hence the solution obtained in practice is mesh dependent. This is of course completely undesirable. It is necessary to mention that the finite element meshes used in practice (if not adaptively constructed) are crude and the FE solution does not show the mentioned effect. For some numerical analysis and computation we refer to [3].

3) The problem of the built in plate (beam).

Let us consider the classical problem of an infinite plate problem (in 2 dimension) which can be formulated as two dimensional (plane strain) problem in the coordinates xy. The scheme of a concrete example is shown in the Fig.3.1 where we assume built in (clamped) boundary conditions.
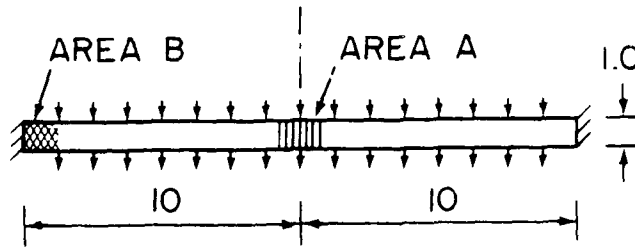

Fig.3.1 The scheme of the considered plate.

We define once more *the basic problem* as the two dimensional elasticity problem with $\nu = 0.3$ (where we denoted by ν the "Poisson ratio") and with the modulus of elasticity $E = 3.10^7$. The built-in (clamped) boundary condition is modeled by $u = v = 0$.

The solution e::ists, and is unique. Assume that the *aim* of the analysis *are the stresses* in the areas A and B shown in Fig. 3.1. Let us further distinguish 2 cases for the data of interest

a) the bending moment and the shear force

b) maximal stresses and the stress distribution through a cross section.

3.1. The problem of the boundary conditions.

It is obvious that the modeling of the clamped end *is an idealization*. In reality the support is obviously more complex. Hence we have an uncertainty in the formulation of the boundary condition and the problem shown in Fig.3.1 can be understood as the simplified one. To analyze this

8

problem consider a few configurations which could be expected to lead the same simplified problem. They are shown in Fig.3.2.
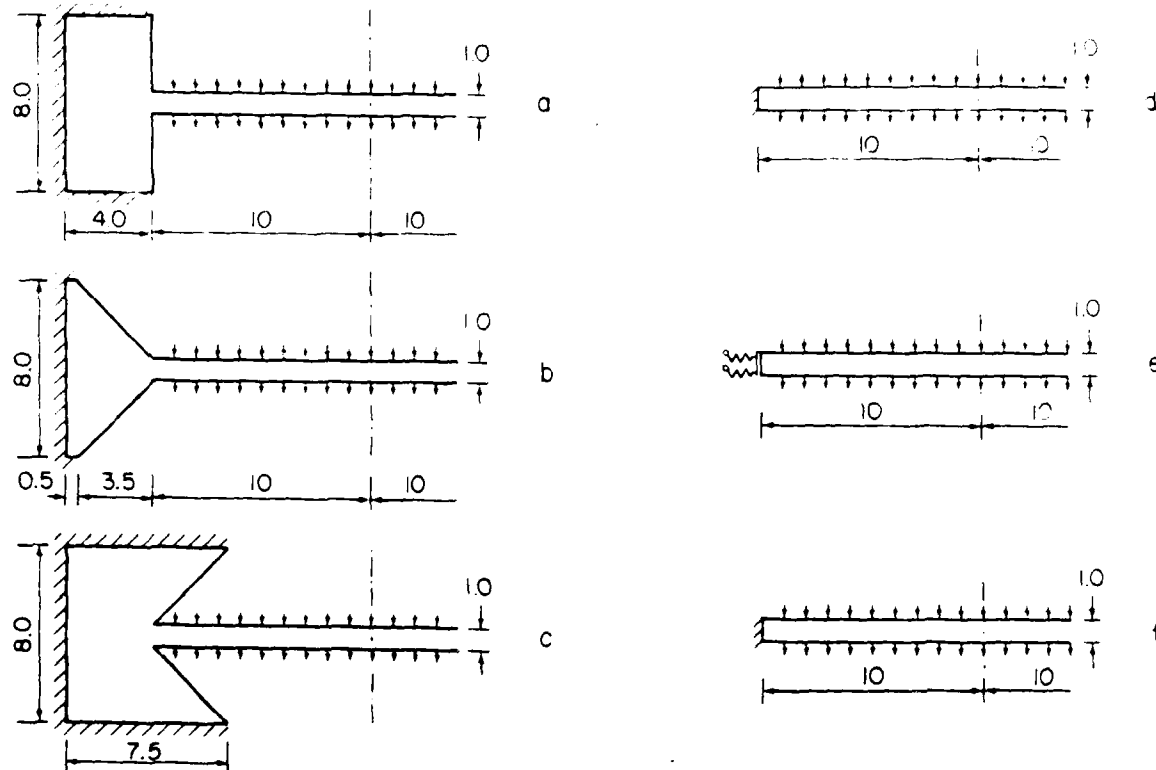

Fig.3.2   The scheme of various boundary conditions.

In the case (e) we model the clamped end as the elastically built-in end. The boundary conditions are then

$$T_x = -cv$$

$$T_y = -cw$$

where $c = 10^8$.

The case (f) depicts a still further simplified problem based on the Kirchhoff beam theory (strength of material approach). In this case the value of the bending moment in the center is

(3.1)
$$M = \frac{1}{24} \, 10^2 = \frac{100}{6}$$

9

Assume first that we are interested in the maximal stress σ_x *in the center of the beam* (area A in Fig.3.1). We get then in the case f : σ_x = 100.

We let the stress σ_x = 100.23 in the case d) (i.e. the case shown in Fig.3.1) be the "exact" solution to which we will compare all others. Table 3.1 shows the results.

Table 3.1. The stresses at the center for various models.

Case	σ_x	Error
a	108.46	8.2%
b	109.76	9.5%
c	108.27	8.0%
d	100.23	0%
e	120.17	19.9%
f	100.00	0.2%

Table 3.1 shows that simplification of either problem a,b,c leads to the error about 10% while the simplification of the case d by Kirchhoff hypotheses leads to error of 0.2%.

We have considered the special case for the ratio $d/L = \frac{1}{20}$. If d $\rightarrow$ 0 (for fixed L), the relative difference between the cases a,b,c, and d goes to zero. We have then

In the case a):

(3.2) $$\alpha_{ad}(d) = \frac{|\sigma_x^a - \sigma_x^d|}{|\sigma_x^d|} = c_1 d + \text{higher order terms}.$$

For $d/L \le \frac{1}{20}$ we can neglect in (3.2) the higher order terms. Table 3.2

shows that in fact $\alpha_{ad}(d) = c_1 d$ with high accuracy.

Table 3.2 . The relative error $\alpha_{a,d}(d)$ of the case a with respect to the case d

d/L	$\alpha_{ad}(d)$
1/20	8.2%
1/50	3.2%

Let us now consider simplification of the problem d to the problem f. We have then

$$\beta_{df}(d) = \frac{|\sigma_x^d - \sigma_x^f|}{|\sigma_x^d|} = c_2 d^2 + \text{higher order terms.}$$
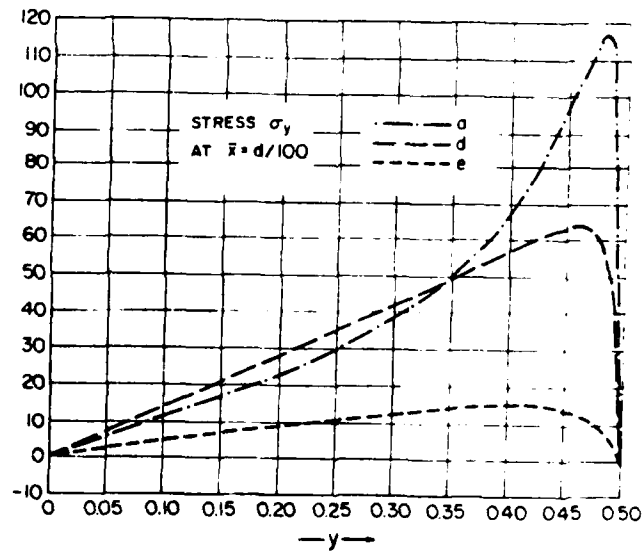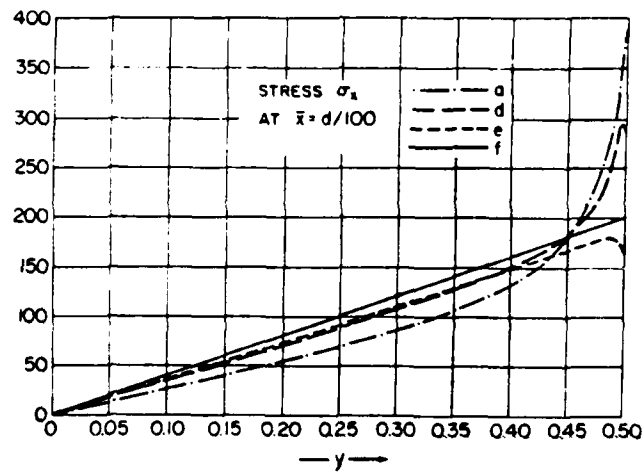
We see that the error of the modeling of the boundary conditions is much more significant than the error of the simplification leading to the Kirchhoff (strength of material) solution.

So far we have computed the maximum of the stress σ_x in the area A. Here the stress is very accurately linear through the cross section and hence when the interest is in the moments, the relative errors mentioned in the table 3.1 and 3.2 hold too.

We reported the stress in the area A and have seen that the sensitivity to the boundary conditions is of order 10%.

In the area B the differences in the stresses are much larger. The stresses are singular (the singular behavior of the solution will be discussed in the next section). Here we report in the Fig.3.3 a,b,c, the stress in the cross section in the distance $\bar{x} = d/100$ from the boundary. We clearly see that the differences between the mentioned cases are significant. On the

11

other hand let us be interested in the (bending) moment and shear force. Then using equilibrium condition we easily see that the differences in the moments are the same as in the center of the beam i.e. as in the area A. Hence different aims lead to very different sensitivities to the uncertainties in input data.
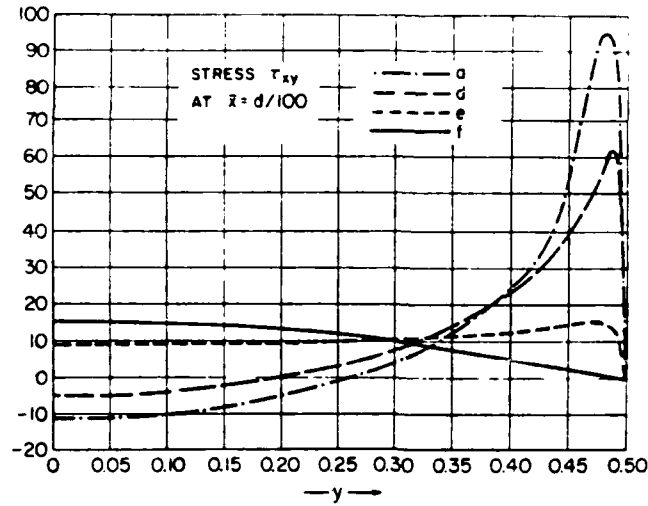
Fig. 3.3   The stresses in the area B.

4) The singularity problem and zooming principles.

4.1   The problem in 2 dimensions.

Let us consider the linear elasticity problem on a polygon domain Ω with the boundary consisting of straight segments Γ_i, $i = 1,\ldots,n$ and vertices $A_i, i = 1,\ldots,n$.   By ω_i we denote the internal angles.   Let us assume that we are dealing with a homogeneous isotropic material and that on every segment Γ_i are boundary conditions with analytic data prescribed and that no volume forces are present.   Then the solution is analytic on $\bar{\Omega}\setminus UA_i$.

The solution is singular in the neighborhood of the vertices.   Let Γ_i, Γ_{i+1} be the segments meeting in the vertex A_i.   Assume for simplicity that the boundary condition (of standard type) are homogeneous on Γ_i, Γ_{i+1}.
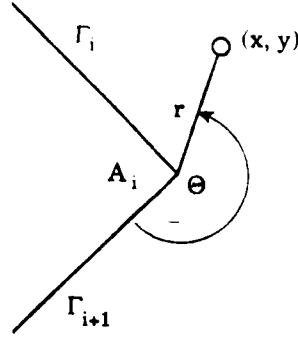
13

Fig. 4.1 Scheme of the angle

Then the solution of the problem in the neighborhood at A_i has the form

$$(4.1) \qquad \left. \begin{array}{c} u(x,y) \\ v(x,y) \end{array} \right\} = \sum_{i=1}^{n} c_i r^{\lambda_i} \left\{ \begin{array}{c} \varphi_i(\theta) \\ \psi_i(\theta) \end{array} \right. + \quad \text{smoother terms}$$

where (r,θ) are the polar coordinates with the origin in A_i as shown in Fig. 4.1. λ_i are real a complex and Re $\lambda_{i+1} \geq \text{Re}\lambda_i > 0$ and φ_i and ψ_i are smooth functions in θ. If λ_i is complex then we use real and imaginary parts separately. Coefficients λ_i and φ_i, ψ_i are given by the geometry (the angle ω_i), the type of boundary condition on Γ_i, Γ_{i+1} and the material properties (in our case Poisson ratio). They are independent of the solution. The coefficients c_i depend *globally* on the solution (except for special cases). The structure of the solution is well known in the general case, for straight and curved segments Γ_i, and for general (linear) materials. We will not go into details. Here we refer instead to [14], [15], [16], [22]. In [21] a general approach (and a computer code) for computation of λ_i, φ_i, ψ_i for anisotropic and nonhomogeneous materials is given. Very often the coefficients c_i called stress intensity factors (together with λ_i, φ_i, ψ_i) are the main aims of the analysis (in 2 and 3 dimensional settings). This is, for example, in the case of design based on the earlier mentioned design code

(USAF-MIL-A-83444). The stresses in the neighborhood of A_i are unbounded when $\mathrm{Re}\lambda_1 < 1$ provided that $c_1 \neq 0$.

Because in finite element computations the stresses are always finite, the character of the computed stresses can be misleading. If $\lambda_1 < 1$ then practically always (except in symmetric cases) $c_1 \neq 0$ although it can be *relatively* small. Then the large stress can be confined to small area only (we will see an illustration in a three dimensional problem in the next section.) *Reliable computational analysis always requires to compute these stress intensity factors.* (For methods of reliable computation of the singular behavior around the corners see references [1], [25]).

Let us now relate (4.1) to the *zooming principle*. To this end let $\xi = \dfrac{x}{\kappa}$, $\eta = \dfrac{y}{\kappa}$, $\rho = \dfrac{r}{\kappa}$ and

$$U(\xi, \eta) = u(\kappa\xi, \kappa\eta)$$
$$V(\xi, \eta) = v(\kappa\xi, \kappa\eta)$$

be the zoomed solution. Then we obviously have

$$(4.2) \qquad \left\{ \begin{array}{l} U(\xi, \eta) \\ V(\xi, \eta) \end{array} \right. = \left\{ \sum_{i=1}^{n} c_i F_i(\kappa) \; \rho^{\lambda_i} \left\{ \begin{array}{l} \varphi_i(\theta) \\ \psi_i(\theta) \end{array} \right.$$

and hence functions $\rho^{\lambda_i}\varphi_i(\theta)$, $\rho^{\lambda_i}\psi_i(\theta)$ are the parts of the zoomed solution with the zooming parameter κ. Here it was characteristic that the infinite sector was invariant with respect to the zooming.

Let us consider now another case, namely the case shown in Fig. 4.2. We can zoom (Fig. 4.2b) the solution at A (see Fig. 4.2a) and get the solution in the form (4.1) (resp. (4.2)) in the same way as before. The other possibility is to zoom the solution with respect to the parameter d as shown in Fig. 4.2b. Then up to rigid body motion the first term in the zoomed solution

15

has the form

$$(4.3) \qquad \begin{matrix} U(\xi,\eta) \\ V(\xi,\eta) \end{matrix} = d^{-1}M \left\{ \begin{matrix} \Phi_1(\xi,\eta) \\ \psi_1(\xi,\eta) \end{matrix} \right. + T \left\{ \begin{matrix} \Phi_2(\xi,\eta) \\ \psi_2(\xi,\eta) \end{matrix} \right. .$$

Here M and T is the moment and shear force at the end of the beam. The function Φ_i, ψ_i, $i = 1,2$ are the functions defined on the domain shown in Fig. 4.2b.
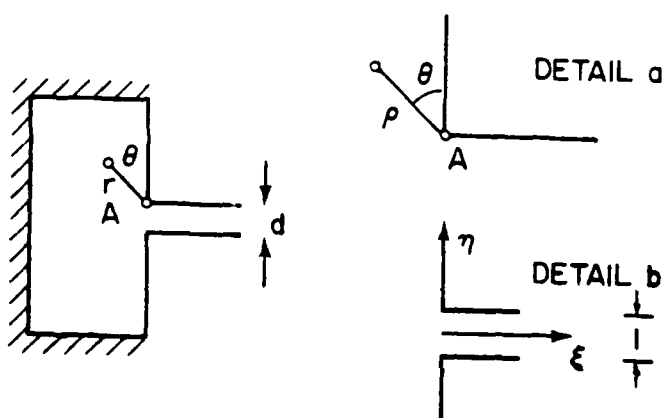

Fig.4.2. The solution on the zoomed domain.

Coefficient M and T are analogous to the stress intensity factors introduced earlier. The zooming principles can be used in many cases when the corner singularity interferes as in the case shown in Fig. 4.2. For more details we refer to [6].

4.3. The problem in 3 dimensions

In 3 dimensions we will consider a polyhedron instead of a polygon and the problem becomes more complex. Once more we will consider the case of isotropic homogeneous maeterial. *Along the edges* the solution is singular in the direction which is perpendicular to the edges and is smooth along the

16

edges. Assuming that the (straight) edge is along the axis z, the singular terms are of the form

$$\left.\begin{array}{c} u(x,y,z) \\ v(x,y,z) \\ w(x,y,z) \end{array}\right\} = c_i(z)r^{\lambda_i} \left\{\begin{array}{c} \varphi_i(\theta) \\ \eta_i(\theta) \\ \zeta_i(\theta) \end{array}\right.$$

where (r,θ,z) are the cylindrical coordinates. Functions $\varphi_i, \psi_i, \zeta_i$ are smooth in θ. There are, in contrast to the two dimensional case, two kinds of singular function. For the first kind coefficients λ_i and functions φ_i, ψ_i are as in 2 dimensions and $\zeta_i = 0$ (they are sometimes called bending singularities). In the second kind we have $\varphi_i = \psi_i = 0$ (and $\xi_i \neq 0$) (they are sometimes called torsion singularities). For details we refer to [15], [22]. The function $c_i(z)$ are the stress *intensity functions* which are smooth in z (except the neighborhood of the verticles).

In addition to the edge type singularity, we have a *vertex singularity*. Here the singular terms have the form

$$\left.\begin{array}{c} u(x,y,z) \\ v(x,y,z) \\ w(x,y,z) \end{array}\right\} = c_i \mathbb{R}^{\Lambda^{(i)}} \left\{\begin{array}{c} \bar{\varphi}_i(\theta,\Xi) \\ \bar{\psi}_i(\theta,\Xi) \\ \bar{\zeta}_i(\theta,\Xi) \end{array}\right.$$

where $(\mathbb{R},\theta,\Xi)$ are the spherical coordinates. Functions $\varphi_i, \psi_i, \zeta_i$ have singular behavior in the neighborhood of (θ_s, ∂_s) being the coordinates of the edges. For details once more see [15], [22].

The coefficient $\Lambda^{(i)}$, and functions $\bar{\varphi}_i, \bar{\psi}_i, \bar{\zeta}_i$ depend on the geometry, boundary conditions and material properties but not on the solution. The coefficients c_i are the analog to the stress intensity factors and depend (except special case) *globally* on the solution. The relation between λ_i and $\Lambda^{(i)}$ governs the singular behavior of the edge intensity factor function in the neighborhood of the vertex. The unboundedness of the stresses in the

17

neighborhood of the vertex take place when $\Lambda^{(1)} < 1$ provided the coefficient $c_1 \neq 0$. Because of *global* dependence of c_1 on the solution, $c_1 \neq 0$ practically always (except possible in special case of symmetries). Nevertheless c_1 can be small and large stresses can be confined to a small area. Then the usual finite element solution could indicate completely wrong behavior. *Hence computation of c_1 is a necessity to obtain reliable results.*
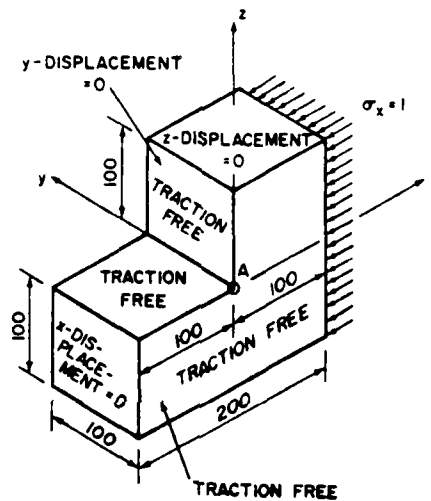

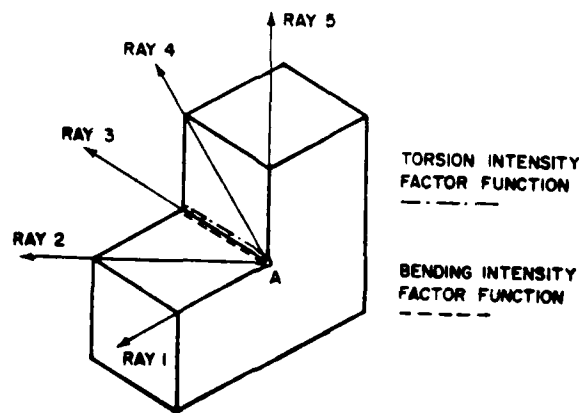Fig. 4.3. The 3 dimensional domain

Fig. 4.4. Location of the rays

Let us show now two typical examples. Fig.4.3 shows a three dimensional domain with imposed boundary conditions. Along the marked edge shown in Fig. 4.4 the stress intensity factor functions are present. In the neighborhood of A solution has vertex type of singularity. In Fig.4.4 we show the rays where the stresses are depicted. The first two coefficients Λ_i are given in Fig.4.5a for $\nu = 0.0$ and $\nu = 0.3$. The stresses on the rays will have then the form

$$\sigma = C_1 R^{\Lambda^{(1)}-1} + C_2 R^{\Lambda^{(2)}-1} + \text{higher order terms.}$$

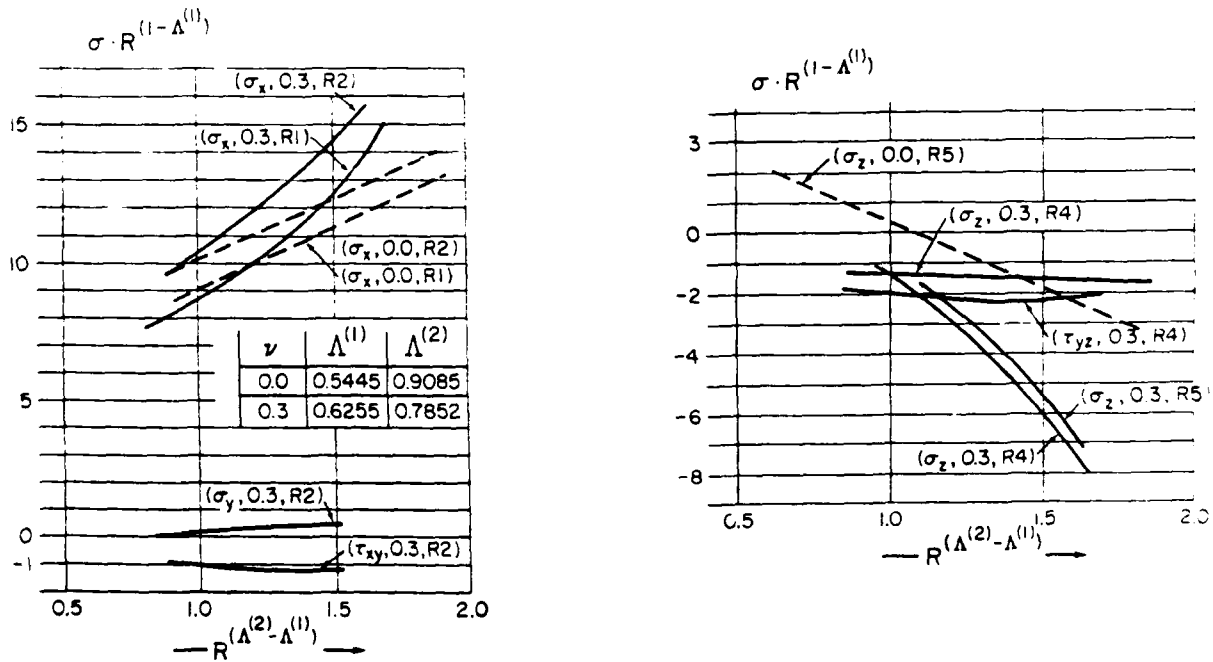| ν	$\Lambda^{(1)}$	$\Lambda^{(2)}$
0.0	0.5445	0.9085
0.3	0.6255	0.7852

Fig.4.5. The behavior of stresses on the rays.

and

$$\sigma R^{1-\Lambda^{(1)}} = C_1 + C_2 R^{(\Lambda^{(2)}-\Lambda^{(1)})} + \text{higher order terms.}$$

Hence in the scale $\sigma R^{1-\Lambda^{(1)}} \times R^{(\Lambda^{(2)}-\Lambda^{(1)})}$ the behavior is linear for small

R. C_1 and C_2 relate to the need to compute two *stress* singular functions.
Fig. 4.5 ab depict the stresses on different rays. The Fig. 4.5ab show well
also the scales where the large stresses will appear (which is of the order of
1/100 of the thickness). We also see that the value of ν does not signifi-
ntly influence the behavior of the solution. Nevertheless this is not always
the case as we will see in the next example.

The second problem (which was suggested by K. J. Bathe, (see also [9]) is
depicted in Fig. 4.6.

Fig. 4.6   The Bathe's problem

The boundary conditions are shown in the figure. When nothing is explicitly
stated then the associated tractions are zero. Let us consider now the
behavior of the solutions at the edge   I-A: for $\nu = 0.0$ and $\nu = 0.3$.
The values of the constants $\Lambda^{[1]}$ are the same as in the previous example.
Fig. 4.7 shows now the stress σ_x at the edge   I-A. We see here drastic
difference between the stress behavior for $\nu = 0.0$ and $\nu = 0.3$. The
standard finite element analysis will lead to the conclusion that σ_x is
bounded on the edge I-A for $\nu = 0.3$ while for $\nu = 0.0$ is large. This
conclusion is of course completely wrong. Let us mention that the strength of
material solution predicts $\sigma_x = -280$ for $x = -d$ and $z = 0$. This value

is approximately achieved for $\nu = 0.0$ for any y (the problem here is
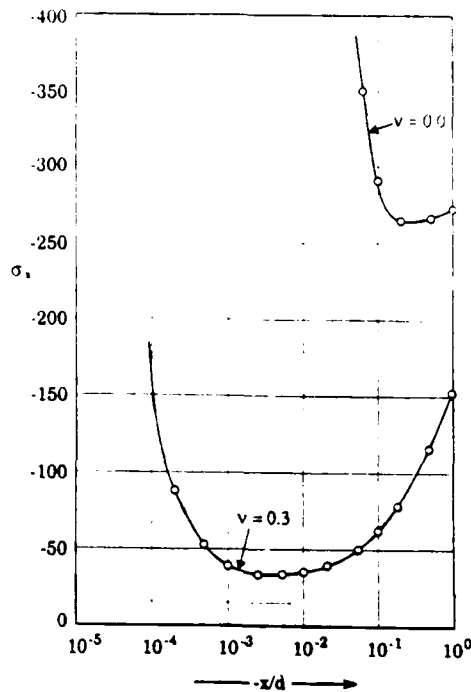

Fig. 4.7   The stress σ_x on I-A for $\nu = 0.0$ and $\nu = 0.3$

y-independent). For $\nu = 0.3$, it is approximately achieved for $y > 7d$[*].

We see that for a reliable conclusion about the stresses in the neighborhood

of the corners and edges the computation of the stress intensity factor *is*

essential and any program should always have to be able to provide them

(STRIPE provides them). For more about the problem of reliable computations

in solid mechanics and detailed analysis of Bathe problem and engineering we

refer to [1].

5.   The plate problem

The plate (and shell) problem is a basic problem in engineering. As the

basic mathematical problem we will understand the three dimensional problem

of elasticity on the thin domain

---

[*]Analysis of the problems of this section has been made by programe STRIPE by
Dr. B. Andersson.   For more see also [1].

$$\Omega = \{x,y,z \mid (x,y) \in \omega, \; |z| < d/2\}.$$

We will assume isotropic homogeneous material.

5.1 The problem of the derivation of the simplified formulation.

There are very many formulations of the plate problems. For the survey see [20] [23]. The major simplified formulations are the Kirchhoff [K] and Reissner-Mindlin (RM) formulations. Many results describe the asymptotic behavior of the solution of 3 dimensional (basic) formulation as $d \to 0$. These results show that (for example in the energy norm) the 3D and Reissner-Mindlin solutions converge to the Kirchhoff solution as $d \to 0$, see eg. [12], [19]. For a detailed study of the asymptotic behavior of Reissner-Mindlin problem we refer to [2].

Further there are generalized models based on the projection in the energy on the space of functions of the form (Kantorovich method)

$$(5.1) \qquad U(x,y,z) = \sum_{k=0}^{n} \varphi_k(x,y)z^k$$

$$V(x,y,z) = \sum_{k=0}^{n} \psi_k(x,y)z^k$$

$$W(x,y,z) = \sum_{k=0}^{m} \xi_k(x,y)z^k.$$

In the case $\nu = 0$, the case $n = 1$ with $\varphi_0 = \psi_0 = 0$ and $m = 0$ leads to RM model. For $\nu > 0$, $n = 1$, $m = 2$, $\varphi_0 = \psi_0 = \xi_1 = 0$ leads to RM model with singular perturbations. Usually $m = n+1$ is taken, which guarantees the proper asymptotic rate of convergence. The model based (5.1) will be called n-m model. In general n and m can be different in different parts of ω. For $n,m \to \infty$ the solution of (n-m) model converges to 3 dimensional solution (in the energy norm).

22

The form (5.1) leads to a hierarchic family of models. It depends on particular choice of the function in z. In (5.1) polynomials have been used. This choice is optimal in an asymptotic way when $d \rightarrow 0$ (see e.g. [12], [26]). Other optimal choices can be considered too [24].

The error of the various models have to be judged in the relation to the 3D *solution* and which data are of interest.

5.2 The problem of the rhombic simply supported plate.

Let us consider the plate shown in Fig.5.1. The simple support can be formulated as

a) hard simple support
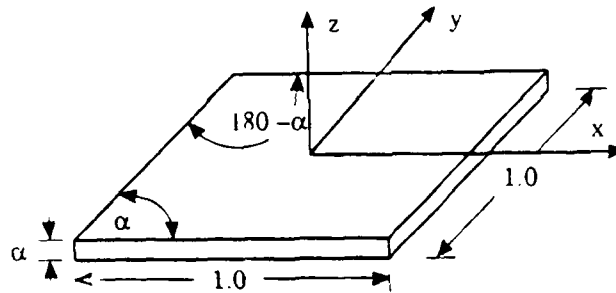
b) soft simple support

Fig. 5.1 The rhombic plate

In the case a) we assume on the lateral sides $w = 0$ and $u_t = 0$ where by u_t we denote the displacement in the directions of the tangent to the boundary of ω (and hence $T_t \neq 0$), u_n is free (i.e. $T_n = 0$).

In the case b) the only constraint on the lateral side is $w = 0$ (and hence $T_n = T_t = 0$). The K-model cannot distinguish between these two supports. Few problems now appear

i) How much do the solutions for the two models of support differ?

ii) Which support does the K-model describe?

iii) How accurate (with respect to the 3D model) are the K and RM models?

Answers to these questions depend strongly on how we measure the error. It is well known that the major difference between K and RM model is in *the boundary layer*. For a detailed analysis in the case when the boundary of ω is smooth we refer to [2].

If we take the energy norm measure of the error and the load uniform on the upper side of the rhombic plate the relative error in % for the K-model, and the m = n = 2 model (which leads to the slightly smaller error the RM model) and for the *soft simple support* is given in Table 5.1 (3D solution is taken as exact).

Table 5.1 The relative energy norm error of K and m = m = 2 model for soft simple support in %

α	$\nu = 0.0$				$\nu = 0.3$			
	d = 0.1		d = 0.01		d = 0.1		d = 0.01	
	K	(2,2)	K	(2,2)	K	(2,2)	K	(2,2)
90°	39.56	12.57	11.87	3.50	34.52	11.18	9.88	2.94
80°	39.91	12.59	12.23	3.57				
60°	42.24	12.72	15.46	4.14				
40°	45.43	13.60	20.50	4.24				
30°	48.27	15.41	22.66	4.34	44.68	15.03	18.91	3.68

Table 5.2 shows for α = 90 and $\nu = 0$ the error for the hard support (the 3D solution with hard support is taken as exact). The error of the 3D solution with the hard support with respect to the soft support of 3D formulation is 34.7% for d = 0.1 and 11.7% for d = 0.01 For more see [19].

24

Table 5.2   The relative enery norm error for the K and (2.2) model
            for hard support in %.

Model	d = 0.1	d = 0.01
K	20.31	2.03
(2.2)	8.22	0.68

The difference between models eg. K, RM, n-m and 3D model is largest in

the boundary layer.   It can be in fact very large.

To illustrate this, we consider the square plate (α = 90, ν = 0.0).   Let

Q_{xz} and Q_{yz} be the shear forces on the line x = 0.5, 0 < y < 0.5 computed

from the 3 dimensional solution for d = 0.01 and soft support.   They are

shown in Fig.5.2ab.   Realizing that the K-model leads to Q_{yz} = 0, we see that

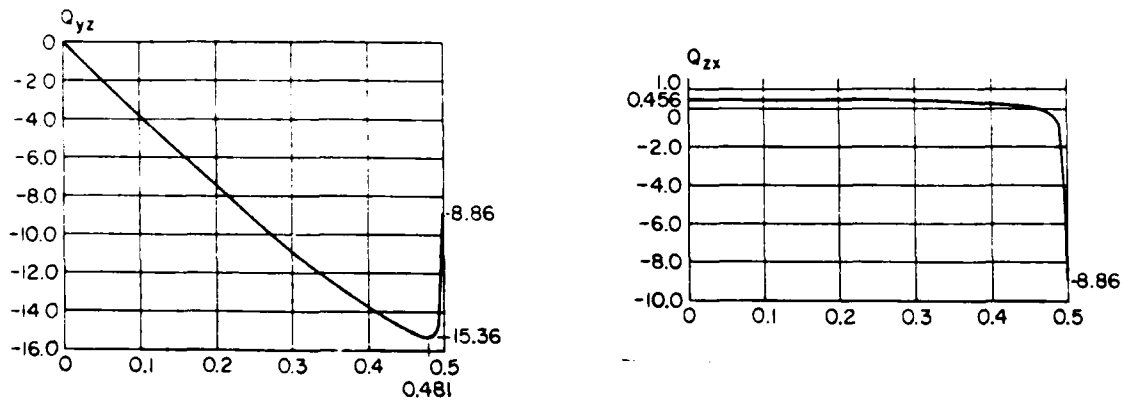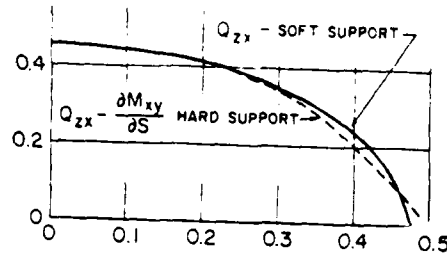K-model is unreliable for these data of interest.

Fig.5.2 The shear force Q_{xz} and Q_{yz} at x=0.5 and 0<y<0.05

The K-model approximates relatively well the *hard support* but not the

soft one.   In the larger distance from the boundary, the K-model is usually

usable also for the soft support.   Although the K-model approximates the hard

support the usual approach is to modify the reaction Q_{xz} by the derivative of

the twist moment to get the soft support reaction.   This leads to a reasonably

good approximation of Q_{xz}. In Fig.5.3 Q_{xz} for soft and hard support with twist moment adjustment is shown. Nevertheless no adjustment of K-model could give reasonable values of Q_{yz}.

5.3 The reaction Q_{xz}.

There is a significant theoretical difference between hard and soft sample support.

In [6] we have analyzed the behavior of the solutions on a regular n-eck polygons ω_n inscribed in the unit circle. We have shown that for hard simple support the solution in ω_n converge to a solution on the circle S but which paradoxically *is not* the solution on S for the hard simple support. This happens for K, RM and 3D model. In contrast, in the case of the soft support, such paradox does not occur. This shows that the mathematical problem of the hard support has a property which we would not expect in "reality" and hence an increased precaution has to be given when hard support model is used.

5.2 The problem of the solution singularity of the plate models.

Let us once more consider the square plate ($\alpha = 90°$), $d = 0.01$, $\nu = 0.3$ such that the sides $0.5 < x < 0.5$, $y = \pm 0.5$ *are clamped* ($u,v,w = 0$) and other two sides *are free*. Then in the neighborhood of the vertices the solution is singular. In [11], [27] the singular behavior of the RM solution

26

is analyzed. This analysis shows that RM solution has two different characters of the singularities. Denote by (r,θ) the polar coordinates with center in $A = (0.5, 0.5)$. Then for $r \ll d$ the solution for example the stresses or moments have the form

$$M_x \cong \sigma_x \cong Cr^{\lambda_{RM}} \varphi_{RM}(\theta)$$

while for $r \approx d$, the singularity is as for the Kirchhoff model

$$\sigma_x \cong Cr^{\lambda_K} \varphi_K(\theta)$$

Between these two areas there is a transition domain. The exponents λ_{RM}, λ_x satisfy some transcendental equations. In our case

$$\lambda_{RM} = -0.241$$

$$\lambda_K = +0.0686 + i0.438$$

(i.e. the stress of K-solution is oscillating). In Fig. 5.4 we show the stress σ_x at the diagonal of the plate in log - log scale. We see clearly that both types of singularities occur. Other stresses show similar behavior.
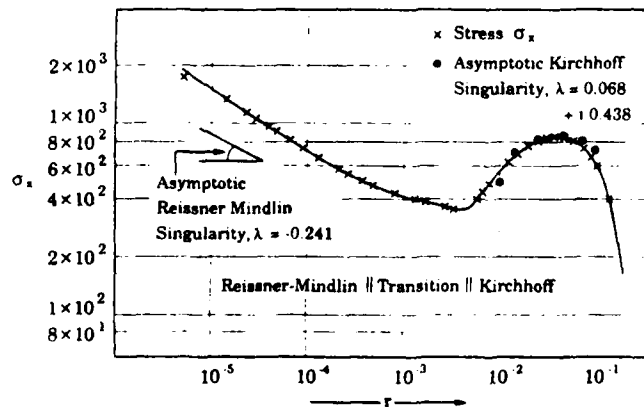

Fig. 5.4 Stress σ_x of the RM model.

Finally we can compute the character of the moments computed from the 3 dimensional solution. Here we can show that

$$M_x \approx Cr^{\lambda_{3D}} \varphi_{3D}(\theta)$$

and in our case

$$\lambda_{3D} = -0.289$$

We see that the corner behavior is different for these 3 models. This difference strongly depends on the geometry of the plate and boundary conditions. For more we refer to [8].

6.   The problem of nonlinear elasticity

The nonlinear formulation in the theory of elasticity stems from

a) nonlinear geometry as large displacements, stresses, etc.

b) nonlinear constitutive law.

Here we will address some questions related *to the elasticity* assuming static behavior where effects of velocity etc. can be neglected. In *one dimensional case*, given the strain $\varepsilon(t)$ $-\infty < t < \infty$ the constitutive law leads to the stress response $\sigma(t)$

(6.1) $$\sigma = A\varepsilon$$

where A is an operator mapping the strains into the space of stresses.

In the 3 dimensional case, ε and σ are the strain and stress tensors, respectively.

Usually the constitutive law in 2 and 3 dimensions is derived from the one dimensional law by applying various principles as Mises, Tresca, Huber-Hencky, etc. In one dimension many laws were proposed, see e.g. [28]. The basic laws are kinematic, isotropic hardening and others. Recently the formulation by Chaboche [13] has become popular.

Mathematically it is important that the constitutive law is such that it satisfies conditions which guarantee the desirable properties of the mathe-

matical problem of elasticity where it is used. It is of course also important that there is not a large difference between observed and predicted response (based on the constitutive law used).

6.1 Experimental results

Results of an extensive one dimensional, experimental analysis with the aluminum alloy 5454 in the H32 condition are reported in [18]. This alloy is produced (under the same commercial mark) by different manufacturers and is widely used in engineering.

The analysis in [18] is based on the fact that in engineering the material is taken from the warehouse and at best the experiments for selection of the proper constitutive law can be made on samples only (statistical approach). Hence 84 samples have been taken and analyzed. Among others, the main questions were related to

    a) reproducibility of the response

    b) selection of the constitutive law.

Two classes of the strain were considered

    i) the cyclic periodic strain (which is usually used in material science).

    ii) random strain which is more realistic in applications.

The main results can be broadly characterized as follows

    a) The reproducibility factor Q_R for the random strain is of order $\approx 10\text{-}15\%$ where

$$Q_R = \frac{\max_t |A(t) - B(t)|}{\max_t \left| \dfrac{A(t) + B(t)}{2} \right|}$$

Here $A(t)$ and $B(t)$ is the stress response of two different sample to the same *random* strain. For *cyclic* load the factor Q_c is of order 7-10%.

b) For every sample and particular constitutive law mostly used in practice (as Chaboche, kinematic, Mroz, etc.) the constants for the best fit were computed. Then the average value of these (84 samples) were computed and using these constants the constitutive law the factors C_R (resp. C_c) were analogous to Q_R(resp Q_c) i.e. we define

$$C_R = \frac{\max_t |A(t) - \bar{B}(t)|}{\max_t \left| \frac{A(t) + \bar{B}(t)}{2} \right|} \ .$$

Here $A(t)$ is the response for a sample and $\bar{B}(t)$ is the predicted response based on the average constants. For the best law (one of them is Chaboche we get $C_R \approx 22-25\%$ and $C_c \approx 16-18\%$.

For the best fit of one sample we get $C_R \approx 8\%$.

If the set of averaging is small we can get $C_R > 30\%$.

For some laws (in standard use in FE codes), $C_R > 40-50\%$.

In the Table 6.1 we show the $\|\cdot\|_{L_\infty}$ $\|\cdot\|_{L_2}$ norm (in psi) and relative error.

		$\|A-B\|_{L_\infty}$	$\|A-B\|_{L_2}$	$\dfrac{\|A-B\|_{L_\infty}}{\|(A-B)/2\|_{L_2}}$	$\dfrac{\|A-B\|_{L_2}}{\|(A-B)/2\|_{L_2}}$
fd	fq	5322	2334	14.4%	12.9%
fd	Chabache	8346	2654	22.0%	13.5%
fd	Kinematic	11850	3475	32.8%	17.6%

(fd, fq is the label of the sample, Chaboche and Kinematic means response obtained by the Chaboche resp. kinematic law). We mention that for computational purpose, the norm $\|\cdot\|_{L_\infty}$ is essential (and not $\|\cdot\|_{L_2}$).

As an illustration we show in Fig. 6.1, 6.2, 6.3, the value for A-B (two

samples) and A-B̄ for character and kinematic law using average constants, for
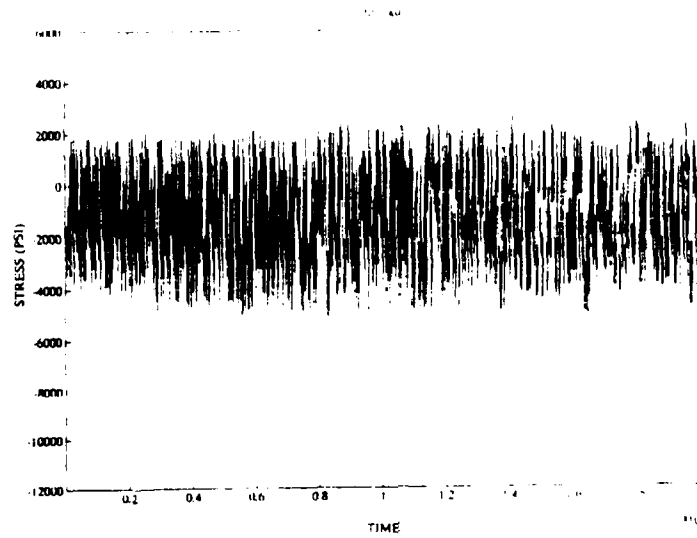the random strain.
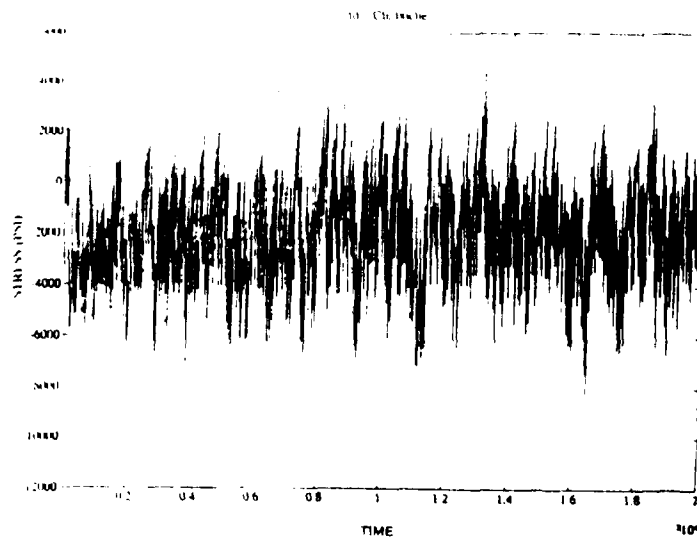

Fig.6.1   The difference between two samples

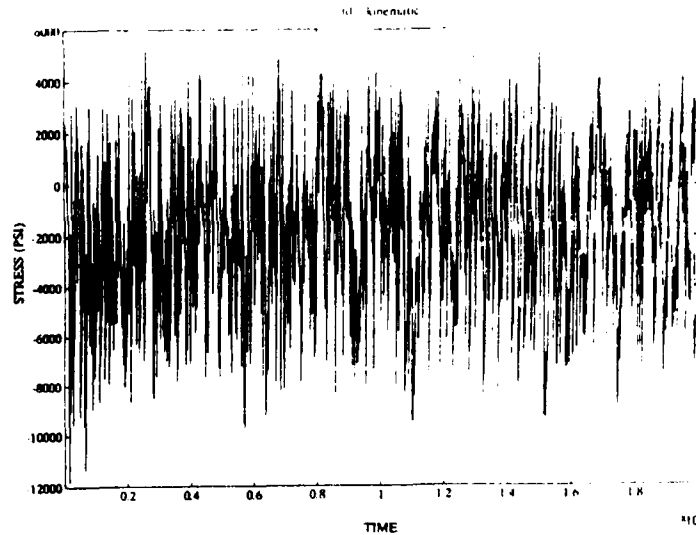Fig.6.2   The difference between sample and Chaboche law

31

Fig.6.3 The difference between sample and kinematic law.

[18] analyzes only the one dimensional problem. It is possible to expect that in 2 resp. 3 dimensional setting the factors will be larger.

The analysis made in [18] indicates

a) It is necessary to analyze the reliability of constitutive laws derived from statistical sampling.

b) It is necessary to analyze random and not cyclic strains.

c) It is highly desirable to develop a mathematical theory for determining the constitutive law based on the (infinitely dimensional) identification problems and to develop a strategies for optimal selections of strains for experiments. This is especially important for 2 and 3 dimensional settings.

d) It seems that the usual elasticity formulation and computation based on the "average" constitutive law cannot give reliable results and other approaches such as bracketting have to be developed, see also here [10].

6.2 Mathematical formulation of Chaboche law.

We have seen in the Section 6.1 that the Chaboche law is one of the laws which fits best the data for the single sample. Therefore we will discuss it here in more detail.

Although in [13] the law is formulated in an incremental way related to mechanical interpretation, it can be cast into a system of ODE for the stress and *two* (internal) parameter functions, $(\sigma(t), \chi(t), R(t))$ for given strain $\varepsilon(t)$. In what follows we denote $\dot{\varepsilon}(t) = \dfrac{d\varepsilon}{dt}$ etc. The Chaboche law is characterized by 6 constants.

We have

$$\dot{\sigma} = E\dot{\varepsilon}, \qquad\qquad \sigma(0) = \chi(0) = R(0) = 0$$

$$\dot{\chi} = 0, \qquad\qquad \varepsilon_h(0) = \varepsilon_y, \; \varepsilon_\ell(0) = -\varepsilon_y$$

(6.2)
$$\dot{R} = 0$$

$$\dot{\varepsilon}_h = 0$$

$$\dot{\varepsilon}_\ell = 0$$

for all $t \in \mathcal{S}$, where

$$\mathcal{S} = \{t \mid \varepsilon_\ell(t) < \varepsilon(t) < \varepsilon_h(t), \text{ or } \varepsilon(t) = \varepsilon_h(t)$$

$$\text{and } \dot{\varepsilon} \le 0 \text{ or } \varepsilon_\ell(t) = \varepsilon(t) \text{ and } \dot{\varepsilon} \ge 0\}$$

$$\dot{\sigma}(t) = \frac{E[c(a-x(t)) + b(Q-R(t))]}{c(a-\chi(t)) + b(Q-R(t)) + E} \dot{\varepsilon}(t)$$

(6.3)
$$\dot{\chi}(t) = \frac{E[c(a-x(t))]}{c(a-\chi(t)) + b(Q-R(t)) + E} \dot{\varepsilon}(t)$$

$$\dot{R}(t) = \frac{Eb(Q-R(t))}{c(a-\chi(t)) + b(Q-R(t)) + E} \dot{\varepsilon}(t)$$

$$\dot{\varepsilon}_h = \dot{\varepsilon}$$

$$\dot{\varepsilon}_\ell = \dot{\varepsilon} - 2\frac{R}{E}$$

33

for all $t \in P_+$ where

$$P_+ = \{t \mid \overset{o}{\varepsilon} > 0 \quad \text{and} \quad \varepsilon = \varepsilon_h\}$$

and

(6.4)
$$\dot{\sigma}(t) = \frac{E[c(a-x(t)) + b(Q-R(t))]}{c(a+\chi(t)) + b(Q-R(t)) + E}$$

$$\dot{R}(t) = \frac{tb(Q-R(t))}{c(a+\chi(t)) + b(Q-R(t)) + E}$$

$$\dot{\varepsilon}_h = \dot{\varepsilon} - 2\frac{R}{E}$$

$$\dot{\varepsilon}_\ell = \dot{\varepsilon}$$

for all $t \in P_-$, where

$$P_- = \{t \mid \overset{o}{\varepsilon} < 0 \quad \text{and} \quad \varepsilon = \varepsilon_\ell\}$$

Chaboche model is characterized by 6 constants with a physical interpretation.

a: Kinematic coefficient

c: Kinematic exponent

Q: isotropic exponent

b: isotropic exponent

g: yield strain

E: elastic modulus

The Chaboche law as formulated can be generalized into 2D and 3D formulations. Nevertheless when this is used in the nonlinear elasticity equation problem, some desirable mathematical properties of the problems (as for example, the existence of the solution) are not quaranteed. Hence another formulation which approximate well the Chaboche law and leads to the desirable properties of the mathematical formulation should be used.

6.3 A proper mathematical formulation of the constitutive law.

Let us outline now here principles and family of constitutive laws (called gauge method) which guarantee good properties of the mathematical problems based on them. There are two basic (sufficient) conditions for it.

a) Existence and convexity of the yield surface

b) the normality condition

(These conditions are related to the Druckers postulates).

Let $\underline{\alpha} \in \mathbb{R}^m$ be the set of internal parameters, $\underline{\alpha} \subset A \subset \mathbb{R}^m$, A being a convex set in $\mathbb{R}^m$. Set further $\sigma \in \mathbb{R}^3$ (for a two dimensional problem).

Now we will formulate the law with the help of the yield function. To this end let $F(\sigma, \alpha)$, $F : \mathbb{R}^3 \times A \rightarrow R$ be given so that

(6.8a) F is convex and C^1

(6.8b) $F(0,0) = 0$

(6.8c) There exist constants γ, Γ such that $0 < \gamma < |\delta_\alpha F||\delta_\alpha F| < \Gamma$

uniformly on the set $\{(\sigma, \alpha)|F(\sigma, \alpha) = z_0\}$ for some z_0.

Then

(6.9) $\dot{\sigma} = D\dot{\varepsilon}$ if $t \in \mathcal{E}$

$\dot{\alpha} = 0$

(6.10) $\dot{\sigma} = \left[D - \dfrac{D\delta_\sigma F(\delta_\sigma F)^T D}{(\delta_\alpha F)^T(\delta_\alpha F) + (\delta_\sigma F)^T(\delta_\sigma F)} \right] \dot{\varepsilon}$

$\dot{\alpha} = - ((\delta_\alpha F)^T - (\delta_\alpha F))^{-1}((\delta_\sigma F)^T \dot{\sigma})\delta_\alpha F$ if $t \in \mathcal{P}$

where

$\mathcal{E} = \{t|F(\sigma, \alpha) < z_0$ or

$F(\alpha, \alpha) = z_0$ and $(\delta_\alpha F)^T \dot{\sigma} \leq 0\}$

35

$$\mathcal{P} = \{ t \mid F(\sigma, \alpha) = z_0 \quad \text{and} \quad (\delta_\sigma F)^T \dot{\sigma} \geq 0 \}.$$

The Chaboche model could be cast approximately in the above frame using

$$F(\sigma, \alpha, \beta) = [\max(F_1(\sigma, \alpha. \beta), \ F_2(\sigma, \alpha. \beta)]^*$$

where

(6.10a) $F_1(\sigma, \alpha. \beta) = a_1(\alpha - \alpha_1)^2 + a_2(\alpha - \alpha_1) + a_3(\beta - \beta_1)^2 + a_4(\beta - \beta_1) + (\sigma - \sigma_1) + \zeta_1$

(6.10b) $F_2(\sigma, \alpha. \beta) = b_1(\alpha - \alpha_2)^2 + b_2(\alpha - \alpha_2) + b_3(\beta - \beta_1)^2 + b_4(\beta - \beta_2) - (\sigma - \sigma_2) + \zeta_2$

and [ ]* the smoothing the operator in the neighborhood of the manifold
$F_1(\sigma, \alpha, \beta) = F_2(\sigma, \alpha, \beta)$.

Fig. 6.4a shows the relation between ε and σ for cyclic (sinusoidal) strain with 50 reversals (25 periods) for the constant computed out of the experimental data (averages of Chaboche constants).
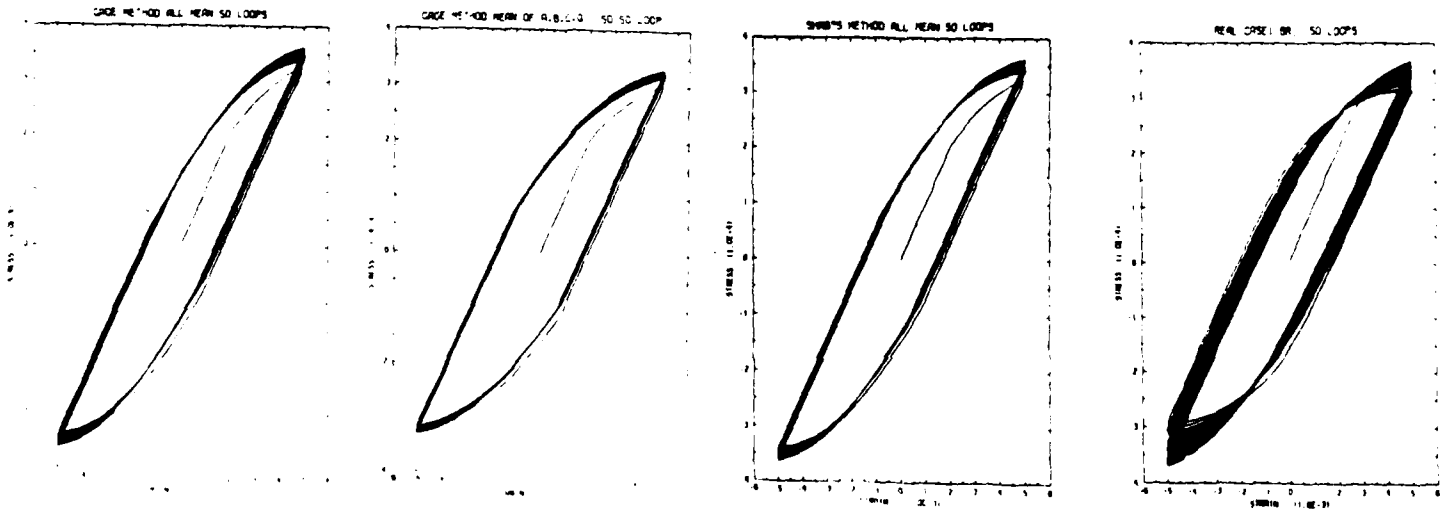

Fig.6.4   The relation between the strain ε and the stress for the law based on (6.10a,b).

Fig. 6.4b shows the results where, for the constant, we have taken the mean minus standard deviation (let us mention that the correlation for these coefficients (see [18]) are of order 0.2). Fig. 6.4c shows the results when computed from the Chaboche law (see section 6.2) and Fig.6.4d shows the experimental results for one sample.

We see that the results from the original Chaboche law are well approximated. In all these data we have assumed that the initial data which depend on past history have been known. In reality they are not known which further increases the uncertainties in the available information. The derivation of 2 and 3 dimensional constitutive law leads to still more uncertainties because not enough experiments could be made. In [10] the 2 dimensional constitutive law was derived as the limit of the frame made out of the bars, analogous Cauchy's derivation of linear elasticity.

We have seen that the computation of the problem of elasticity on the assumption of the knowledge of constitutive law without respecting the uncertainties leads to unreliable results.

7.   A posteriori error analysis of the model.

It is essential to make a posteriori analysis of the error of the solution of the simpliefied problem when only the data from this simplified model are used. This can often be made by two sided energy estimates. For details see e.g. [17].

7.1.   Estimate of the error of geometry idealization.

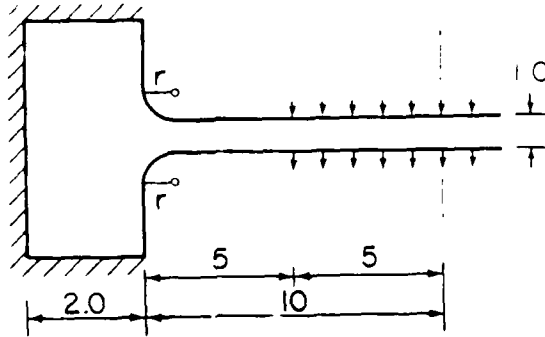Consider the problem on Ω_r shown in Fig. 7.1.

Fig. 7.1. Scheme of the problem with perturbed boundary.

Let the basic mathematical problem be the 'inear elasticity on Ω_r and the simplified problem is the problem on Ω_0 using $E = 1$, $\nu = 0.3$ (and $r = 0$). Then by finite element solution we get two stress intensity factors (see Section 4) $c_1 = 0.2157 \ 10^2$, $c_2 = 0.5929 \ 10^2$. Then the estimate using c_1, c_2 (and the form of the singular functions) allows to compute the upper estimate in the energy norm on Ω_0 of the difference between the solutions on Ω_r and Ω_0 (see [17]). Table 7.1 gives the results together with the true error obtained by the solution on Ω_r.

Table 7.1 The estimate and true error of the geometry ideal

r	Estimate	True error
0.1	19.0%	13.2%
0.01	3.5%	3.0%

We see good effectiveness of the estimate.

7.2 Estimates of the linearization

Let us consider once more the problem shown on Fig. 7.1 with $r = 0$. If the simplified problem will be understood as the linear problem the strains and stresses are infinite (see Section 4). If we would consider as the basic

38

problem the nonlinear problem, the nonlinearity will occur in the neighborhood of the corner. We will assume the Hencky model of the nonlinear elasticity with the governing function

$$\varphi(\zeta) = \begin{cases} \zeta & \text{for } 0 \le \zeta \le \zeta_0 \\ \beta\zeta + \dfrac{1-\beta}{\gamma}\zeta_0^{1-\gamma}\zeta^\gamma - \dfrac{(1-\gamma((1-\beta))}{\gamma}\zeta_0 & \text{for } \zeta > \zeta_0 \end{cases}$$

with $\gamma \in \left[\dfrac{0.5-\beta}{1-\beta}, 1\right)$.

Functions $\varphi(\zeta)$ is the function describing the nonlinearity of the material.

Let us consider the problem depicted in Fig.7.1 with $E = 10^6$, $\nu = 0.3$. Table 7.2 shows the upper estimate of the relative error mentioned in the energy norm for various values of β, γ, ζ_0. For more details we refer to [17].

$\zeta_0 = 0.01$			$\zeta_0 = 0.001$		
β	γ	Estimate of relative error	β	γ	Estimate of relative error
0.1	0.501	$2.76 \ 10^{-4}$%	0.9	0.8	$2.05 \ 10^{-5}$%
0.1	0.5001	$2.79 \ 10^{-4}$%	0.9	0.5	$4.06 \ 10^{-5}$%
0.1	0.50001	$2.79 \ 10^{-4}$%	0.9	0.02	$5.36 \ 10^{-5}$%
0.01	0.501	$9.56 \ 10^{-4}$%	0.5	0.8	$1.19 \ 10^{-4}$%
0.01	0.5001	$9.62 \ 10^{-4}$%	0.5	0.5	$2.55 \ 10^{-4}$%
0.01	0.50001	$9.63 \ 10^{-4}$%	0.5	0.2	$3.89 \ 10^{-4}$%
0.001	0.501	$3.03 \ 10^{-3}$%	0.3	0.3	$1.84 \ 10^{-4}$%
0.001	0.5001	$3.07 \ 10^{-3}$%	0.3	0.5	$4.32 \ 10^{-4}$%
0.001	0.50001	$3.08 \ 10^{-3}$%			

8. Conclusions

We have discussed various aspects of reliability without trying to define more precisely what does it mean. We have seen that the aim is to get desired data with an assessment of their accuracy. More precisely we are aiming to get the quantitative bracketts in which the "true" results are. These bracketts then express the uncertainty of the results caused by uncertainties in the input data, the (simplified) formulation, the discretization etc.

We can now roughly define the reliability of engineering computations in the *relation to reality*.

The computational results furnished with the bracketts are physically reliable if the physically observed results are in the provided bracketts.

Analogously, (more precisely) we can define the reliability of the computational results in *the relation of mathematical analysis.*

The computational results furnished with the bracketts are mathematically reliable if the exact data of the basic mathematical problems are in the provided bracketts.

We have seen that the reliability is related to the data of interest and the definitions what is meant by accuracy (e.g. particular norms) etc.

We have also seen that the mathematical formulation has to be closely related to the engineering analysis and experimentation. Without it, the "physical" reliability is impossible to expect.

The mathematical reliability, i.e. the comparison of the obtained results with the exact data stemming from the *basic mathematical problem* is always (at least in principle) possible. This comparison and its bracketting is then the main goal of the (mathematical) computational analysis.

The reliability of the computational analyses has many features and bring out many unsolved problems. Nevertheless there are already today many

40

ways to get at least partial *quantitative* insight into reliability of computed results.

REFERENCES

1. B. Andersson, I. Babuŝka, U. Falk T. Petersdorff, Accurate and Reliable Computation of Complete Solutions of Equations of Linear Elastomechanics on Three-dimensional Domains, to appear.

2. D.N. Arnold, R. Falk, Edge Effects in the Reissner-Mindlin Plate Theory, Preprint, Symposium on Analytical and Computational Methods for Shells, December 1989, San Franciso, to appear in Proceedings of Am. Soc. of Mech. Engineers.

3. I. Babuŝka, Uncertainities in Engineering Design, Mathematical Theory and Numerical Experience, in J.A. Bennett and M.E. Botkin, eds. The Optimum Shape pp.171-197, Plenum Press, New York 1986.

4. I. Babuŝka, J. Pitkäranta, The Plate Paradox for Hard and Simple Support. SIAM J. Math. Anal. 1990.

5. I. Babuŝka, A. Miller, The Postprocessing Approach in Finite Element Method, Int. J. Num. Meth. Engrg. 20 (1984), 1085-1109, 111-1129, 2311-2324.

6. I. Babuŝka, T. Petersdorff, Boundary Layers in Beams with Various Boundary Coditions, to appear.

7. I. Babuŝka, T. Scapolla, Benchmark computation and performance evaluation for a Rhombic Plate Bending Problem, Int. J. Num. Meth. Engrg. 28(1989), 155-179.

8. I. Babuŝka, L.Li Corner singularities of the solution of various plate models, to appear.

9. K.J. Bathe, N.S. Lee, M. Bucalem, On the use of hierarchical models in engineering analysis, to appear.

10. E. Bonnetier, Mathematical Treatment of the Uncertainties appearing in the Formulation of some Models for Plasticity. Ph.D. Thesis (1988), University of Maryland, College Park, MD 20742, USA.

11. W.S. Burton, G.B. Sinclair, On the Singularities in Reissner's Theory for the Bending of Elastic Plates, J. Appl. Mech. 53 (1986) pp.220-222.

12. P.G. Ciarlet P. Destuynder, A Justification of the Two Dimensional Linear Plate Model, J. Mécanique 18 (1979), 315-344.

13. J.L. Chaboche, Time Independent Constitutive Theorie for Cycle Plassticity Int. J. of Plasticity 2 (1986), 149-188.

14. M. Costabel E. Stephan, Curvature Terms in the Asymptotic Expansions for Solutions of Boundary Integral Equations on Curved Polygons of Integral Equations 5(1983), 353-371.

15. M. Dauge, Elliptic Boundary Value Problems on Corner Domains. Lecture Notes in Math. 1341, Springer, New York 1988.

16. P. Grisrard Elliptic Problems in Nonsmooth Domains, Pitman, Boston 1985.

17. W. Han. Error Estimations of the Idealization of Mathematical Formulations of Problems Leading to Elliptic Partial Differential Equations, Ph.D. Thesis (1990), University of Maryland, College Park, MD 20742, USA.

18. K. Jerina, I. Babuška Mathematical Modeling of Physical Systems with Considerations of Uncertainities, Washington University, Mech. Engtg. Dept. St.Louis, 1990.

19. D. Morgenstern, Herleitunng der Plattenthearie aus der Dreidimensionales Elastizitätstheorie, Arch Rat Mech. Anal. 4 (1959), 145-152.

20. A.K. Noor, W.S. Burton, Assessment of Shear Deformation Theories for Multilayered Composite Plates, Appl. Mech. Rev. 42 (1989), pp.1-12.

21. A. Papadakis, Computational aspects of Determination of Stress Intensity Factors for Two-dimensional Elasticity, Ph.D. Thesis, (1988), University of Maryland, College Park, MD 20742, USA.

22. T. Petersdorff, Randwertprobleme der Elastizitätstheorie für Polyeder - singularitäten und Approximation mit Randenelement methodem, Ph.D. Thesis (1989), T.H. Darmstadt FRG.

23. E. Reissner. Reflections on Theory of Elastic Plates, Appl. Math. Rev. 38 (1985), pp.1453-1464.

24. C. Schwab. The Dimensional Reduction Method, Ph.D. Thesis (1989), University of Maryland, College Park, MD 20742, USA.

25. B.A. Szabo, I. Babuška, Computation of the Amplitude of Stress Singular Terms for Cracks and reendrant Corners, Fracture Mechanics XIX Symp. ASTM STP 1969, T.A. Cruse ed., Am Soc. Test.and Mat.,Philadelphia, 1987, pp. 101-126.

26. M. Vogelius, I. Babuška, On a Dimensional Reduction Method, Math. of Comp. 37(1981), pp. 31-45, 47-68.

27. D.H.Y. Yen, M. Zhow, On the Singularity of Corner Points of Solutions of Plate Bending Problem, Preprint, Department of Mathematics, Michigan State University, East Lansing, 1989.

28. M. Zyczkowski, Combined Loadings in the Theory of Plasticity, PWN-Polish Scientific Publ. Warsazava 1981.

The Laboratory for Numerical analysis is an integral part of the Institute for Physical Science and Technology of the University of Maryland, under the general administration of the Director, Institute for Physical Science and Technology. It has the following goals:

o   To conduct research in the mathematical theory and computational implementation of numerical analysis and related topics, with emphasis on the numerical treatment of linear and nonlinear differential equations and problems in linear and nonlinear algebra.

o   To help bridge gaps between computational directions in engineering, physics, etc., and those in the mathematical community.

o   To provide a limited consulting service in all areas of numerical mathematics to the University as a whole, and also to government agencies and industries in the State of Maryland and the Washington Metropolitan area.

o   To assist with the education of numerical analysts, especially at the postdoctoral level, in conjunction with the Interdisciplinary Applied Mathematics Program and the programs of the Mathematics and Computer Science Departments. This includes active collaboration with government agencies such as the National Bureau of Standards.

o   To be an international center of study and research for foreign students in numerical mathematics who are supported by foreign governments or exchange agencies (Fulbright, etc.)

Further information may be obtained from Professor I. Babuška, Chairman, Laboratory for Numerical Analysis, Institute for Physical Science and Technology, University of Maryland, College Park, Maryland 20742.